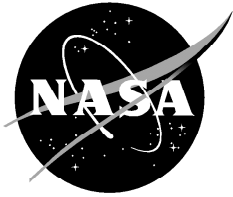


NASA/TM-2001-210392



Developing Uncertainty Models for Robust Flutter Analysis Using Ground Vibration Test Data

*Starr Potter and Rick Lind
NASA Dryden Flight Research Center
Edwards, California*

April 2001

The NASA STI Program Office...in Profile

Since its founding, NASA has been dedicated to the advancement of aeronautics and space science. The NASA Scientific and Technical Information (STI) Program Office plays a key part in helping NASA maintain this important role.

The NASA STI Program Office is operated by Langley Research Center, the lead center for NASA's scientific and technical information. The NASA STI Program Office provides access to the NASA STI Database, the largest collection of aeronautical and space science STI in the world. The Program Office is also NASA's institutional mechanism for disseminating the results of its research and development activities. These results are published by NASA in the NASA STI Report Series, which includes the following report types:

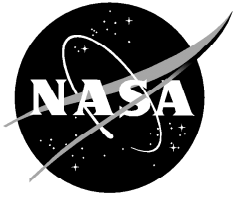
- **TECHNICAL PUBLICATION.** Reports of completed research or a major significant phase of research that present the results of NASA programs and include extensive data or theoretical analysis. Includes compilations of significant scientific and technical data and information deemed to be of continuing reference value. NASA's counterpart of peer-reviewed formal professional papers but has less stringent limitations on manuscript length and extent of graphic presentations.
- **TECHNICAL MEMORANDUM.** Scientific and technical findings that are preliminary or of specialized interest, e.g., quick release reports, working papers, and bibliographies that contain minimal annotation. Does not contain extensive analysis.
- **CONTRACTOR REPORT.** Scientific and technical findings by NASA-sponsored contractors and grantees.
- **CONFERENCE PUBLICATION.** Collected papers from scientific and technical conferences, symposia, seminars, or other meetings sponsored or cosponsored by NASA.
- **SPECIAL PUBLICATION.** Scientific, technical, or historical information from NASA programs, projects, and mission, often concerned with subjects having substantial public interest.
- **TECHNICAL TRANSLATION.** English-language translations of foreign scientific and technical material pertinent to NASA's mission.

Specialized services that complement the STI Program Office's diverse offerings include creating custom thesauri, building customized databases, organizing and publishing research results...even providing videos.

For more information about the NASA STI Program Office, see the following:

- Access the NASA STI Program Home Page at <http://www.sti.nasa.gov>
- E-mail your question via the Internet to help@sti.nasa.gov
- Fax your question to the NASA Access Help Desk at (301) 621-0134
- Telephone the NASA Access Help Desk at (301) 621-0390
- Write to:
NASA Access Help Desk
NASA Center for AeroSpace Information
7121 Standard Drive
Hanover, MD 21076-1320

NASA/TM-2001-210392



Developing Uncertainty Models for Robust Flutter Analysis Using Ground Vibration Test Data

*Starr Potter and Rick Lind
NASA Dryden Flight Research Center
Edwards, California*

National Aeronautics and
Space Administration

Dryden Flight Research Center
Edwards, California 93523-0273

April 2001

ACKNOWLEDGMENTS

The authors would like to thank Cliff Sticht for his invaluable contributions to the Aerostructures Test Wing (ATW) project. He was instrumental in designing the system and developing an associated finite-element model. Additionally, he provided the final updates that were used to match the analytical model with the data. We would also like to acknowledge Tim Doyle and Roger Truax for their support with finite element model updating and flutter analysis. We also thank Mike Kehoe for his ideas towards nonlinearities in ground vibration testing. We greatly appreciate the draft comments provided by Ralph Brillhardt.

NOTICE

Use of trade names or names of manufacturers in this document does not constitute an official endorsement of such products or manufacturers, either expressed or implied, by the National Aeronautics and Space Administration.

Available from the following:

NASA Center for AeroSpace Information (CASI)
7121 Standard Drive
Hanover, MD 21076-1320
(301) 621-0390

National Technical Information Service (NTIS)
5285 Port Royal Road
Springfield, VA 22161-2171
(703) 487-4650

DEVELOPING UNCERTAINTY MODELS FOR ROBUST FLUTTER ANALYSIS USING GROUND VIBRATION TEST DATA

Starr Potter* and Rick Lind†
NASA Dryden Flight Research Center
Edwards, California

Abstract

A ground vibration test can be used to obtain information about structural dynamics that is important for flutter analysis. Traditionally, this information—such as natural frequencies of modes—is used to update analytical models used to predict flutter speeds. The ground vibration test can also be used to obtain uncertainty models, such as natural frequencies and their associated variations, that can update analytical models for the purpose of predicting robust flutter speeds. Analyzing test data using the ∞ -norm, rather than the traditional 2-norm, is shown to lead to a minimum-size uncertainty description and, consequently, a least-conservative robust flutter speed. This approach is demonstrated using ground vibration test data for the Aerostructures Test Wing. Different norms are used to formulate uncertainty models and their associated robust flutter speeds to evaluate which norm is least conservative.

Nomenclature

ATW	Aerostructures Test Wing
FEM	finite-element model
FRF	frequency-response function
FTF	flight test fixture
GVT	ground vibration test

$KEAS$	equivalent airspeed, knots
MAC	modal assurance criterion
n	number
POC	pseudo-orthogonality check
v	estimated mode shape
V_{nom}	nominal flutter speed
V_{rob}	robust flutter speed
	scalar
	uncertainty operator
Δ	set of uncertainty operators
	uncertainty parameter
	analytical mode shape
	set of frequency parameters
	frequency

Introduction

Structural dynamics often are an important consideration when evaluating system characteristics. A concern related to structural dynamics is the analysis of aeroservoelasticity, and particularly the phenomenon of flutter, for a flight vehicle. The instability associated with flutter can be quite sensitive to the structural dynamics; therefore, analysis of robustness with respect to uncertainty is becoming increasingly important for the flight test community. Such an analysis is used to increase flight safety and efficiency factors for envelope expansion of experimental testing.

A ground vibration test (GVT) is commonly performed as a preflight check that attempts to validate the quality of an analytical model and its associated flutter predictions.¹ The basic concept is to excite the structural dynamics and measure responses at locations

* Aerospace engineer, starr.potter@drc.nasa.gov.

† Aerospace engineer, rick.lind@drc.nasa.gov, Member, AIAA.

Copyright © 2001 by the American Institute of Aeronautics and Astronautics, Inc. No copyright is asserted in the United States under Title 17, U.S. Code. The U.S. Government has a royalty-free license to exercise all rights under the copyright claimed herein for Governmental purposes. All other rights are reserved by the copyright owner.

throughout the vehicle. The responses are then analyzed to estimate a set of modal properties for a linear model that corresponds to the observed data. These modal properties, such as natural frequency and mode shape, are compared with an analytical model to ascertain the error and uncertainty in that model.

The modal estimates from a GVT are used to update analytical models; however, updating is often not a straightforward procedure. An accurate procedure for model updating is not yet a solved problem. Several approaches have been formulated to address particular issues of the problem, but fundamental limitations exist to all these approaches. The general difficulties associated with model updating based on measurement data are well-known to the flight test community.²

The concept of uncertainty recently has been receiving attention with respect to model updating. Ground vibration test data must be carefully analyzed because many variations exist in the data as a result of inherent properties of vibration testing.³ Such variability naturally arises from both the process of generating data and the process of analyzing data.⁴ Test procedures can be formulated to reduce the variability,⁵ and orthogonality checks can be conducted during testing to ensure data quality;⁶ however, some variations in measured data will always exist. These variations must be properly treated to ensure that any modal parameters extracted from the data accurately reflect the properties of the structure.

The most common approach to treat variations in experimental data is to consider types of measurement error. One method is to find parameter estimates, or corrections to existing parameter estimates, by minimizing the 2-norm of an error residual based on data with assumed 2-norm bounded measurement uncertainties.⁷ A similar method considers the effect of measurement uncertainties that are modeled using fuzzy set theory.⁸ Another approach is to consider the clustering of pole estimates to minimize the effect of measurement variation on resulting pole estimates.⁹

Methods for data analysis that use mode shape information also exist. In particular, an approach has been formulated that attempts to determine a mode shape to within limits of assumed measurement error.¹⁰ This method perturbs a model with variations that are anticipated to occur as a result of imprecise testing. A model is considered to be accurate to within measurement error if the modal assurance criterion (MAC) of the experimental mode shapes lies within

range of the corresponding criterion for the perturbed mode shapes.

This paper discusses an alternative method of considering variations in data from GVTs. Essentially, the principle here is that no single best answer exists; instead, the objective is to determine an optimal range of possible modal parameters as a result of variation of the data. This approach assumes that determining an exact set of modal parameters from GVT data is not possible, or even mathematically valid. Because inherent nonlinearities and complexities in the structure will always introduce some level of variation of the data, a linear model should always consider that variation.

The approach adopted in this paper is directly related to a particular method of flutter analysis. Linear models are formulated by including uncertain parameters in the dynamics. These parameters are represented by a best-guess nominal value and an associated set of norm-bounded perturbations. A robust analysis is performed on the model by computing worst-case flutter speeds with respect to the uncertain parameters.¹¹ The objective of this paper is to determine the smallest norm-bounded perturbations based on GVT data that result in the least-conservative robust flutter speeds.

The fundamental principles put forth in this paper previously have been recognized as an inherent part of analysis. For example, a concept of choosing methods for data analysis by considering fundamental issues has been discussed in the context of robust reliability for decision making.¹² Essentially, the analysis of uncertainty must be linked with the need to use the result. Similarly, the concept in this paper is to formulate an uncertainty description by considering the need to perform a flutter analysis with respect to that description.

Norm-Bounded Uncertainty

The concept of uncertainty is an intuitively obvious notion as an expression of error and variations in models and data; however, expressing this notion as a mathematical formulation is somewhat more difficult. Several types of mathematical constructions have been proposed to represent uncertainty. These constructions include formulations that reflect properties such as statistical distributions or deterministic measures. A construction should be chosen that accurately reflects the fundamental nature of the uncertainty to be described and also is suitable for the associated robustness analysis to be performed.

Analysis of GVT data to develop uncertainty descriptions is actually performed for the eventual goal of computing robust flutter speeds. These speeds are computed using a mathematical framework based on H_∞ theory; therefore, the uncertainty should be represented as an element in the H_∞ framework.¹¹ Thus, the form for the uncertainty is chosen as a set of stable perturbations formally described as an operator set with finite H_∞ -norm. This type of uncertainty is sometimes noted as sector or interval uncertainty.

The general form used as an uncertainty description is to formulate a set, Δ , that is composed of elements denoted as Δ_i such that $\Delta = \{\Delta_i\}$. Each element is a frequency-varying transfer function that is required to be stable and rational. Furthermore, each element describes a multiple-input and multiple-output system with complex elements.

The range of dynamics admitted into models by the general form of uncertainty is often more broad than is justified by the nature of the errors and variations. For example, physical parameters inherently are real numbers, so allowing complex variations to these parameters seems unrealistic. The analysis of robustness with respect to uncertainty in the H_∞ framework can be overly conservative when considering the general form of uncertainty; therefore, specific subsets of the generalized set of operators are used.

The uncertainty description associated with structural dynamics for the analysis of robust flutter speeds is restricted to affecting the modal parameters of natural frequency and damping. These parameters inherently are real scalars; therefore, the uncertainty is restricted to being real scalars. Furthermore, the variations in each modal parameter are assumed to be independent, so different scalars will be associated with each parameter. The basic description of the uncertainty associated with a modal parameter is given as Δ_i and depends on some real scalar, α_i , greater than 0 to provide a norm bound:

$$\Delta_i = \{ \alpha_i R, | | \} \quad (1)$$

An obvious feature of this type of uncertainty is the numerical distribution of the operators. Specifically, the magnitudes of the operators are symmetrically distributed around 0, which implies that no bias towards either direction, positive or negative, is allowed in the uncertainty. Another feature is the lack of an associated probability distribution. Such distributions are included with descriptions of uncertainty for the purpose of computing statistical robustness.

Statistical robustness analysis typically considers an uncertainty description that relates the probability of operators occurring with all magnitudes. The H_∞ -norm approach is quite different from the statistical method in that this approach considers only operators within a limited range of magnitude. Furthermore, this approach assumes any operator within this range is equally probable and should be analyzed.

Remembering that the uncertainty description is being developed foremost for robust flutter analysis is important. Many types of uncertainty descriptions, such as biased statistical distributions, are not suitable for this application; therefore, this paper focuses on the H_∞ -norm approach.

Ground Vibration Testing

Variability is inherent in GVT data. Some causes for variability of the data in the GVT hardware setup are discussed, as well as its effect on modal parameter estimation.

Variability in Generating Data

A GVT is used to estimate the properties of the structural dynamics before flight operation. A GVT is performed by exciting the aircraft through the application of commanded energy and then measuring the structural motion in response to that energy. For example, a common method of testing aircraft is to connect vibration shakers to the fuselage and wings and measure the responses with accelerometers installed across the vehicle. The data from this testing are analyzed to estimate properties associated with modes such as natural frequencies and the corresponding mode shape. The estimation uses optimization and curve-fit routines to analyze GVT data; therefore, the resulting modal parameters can be overly influenced by variability in the data. Methodical setup and operation of test can help minimize, but never entirely eliminate, such variability.

Variability in data can manifest in several forms. For example, aircraft testing often generates frequency-response functions (FRF). The variability in data associated with an FRF can be noted by frequencies at which peaks occur. For example, different accelerometers may indicate different frequencies at which a bending mode occurs. This variation can be exaggerated when data are collected at different times or by using moving or roving transducers. Other types of variability in FRF data can be noted as differences in amplitudes and damping curves. Amplitude variations can occur as the result of FRF processing techniques or

simply because of transducer calibration variability. Damping variation can be the result of signal processing, including mathematical window application to the data to prevent Fourier transform leakage.

One potentially significant source of variability in GVT data is the process of exciting the structure. Vibration exciters, also referred to as shakers, are commonly used for aircraft testing, but the resulting data are particularly susceptible to variability as a result of poor setup of the shaker. The shaker armature, which is the interface from the shaker to the test structure, can misalign and cause a bending moment input to the force transducer. The effect of this moment is an incorrect measurement of excitation energy and, correspondingly, variability in the amplitude and frequencies associated with peaks in the FRF.

Excitation for vibration testing also can be provided by the use of impact hammers. Different tips and masses are used on impact hammers to control the input frequency spectrum. Increasing the mass on the impact hammer will increase the input force while decreasing the frequency content. Changing the tip stiffness will change the frequency range and peak force of excitation. If the combination of mass and tip stiffness are inadequate, causing a zero frequency component in the frequency range of interest, any measured output acceleration frequency spectrum will not clearly indicate a resonance condition when one is actually present.¹³

The impact test technique can also result in a poor signal-to-noise ratio in the responses of the input and the output. Following the impulse, background noise may become as significant as the signal obtained from the measurement transducers. If the noise level is high enough, the input frequency spectra could result in a frequency shift and peak variation. Impacting a lightly damped structure can cause the output acceleration to continue for much longer than the time sample window. The signal truncation leads to filter leakage. This mismatch in frequency between signal and analyzer frequency components creates magnitude and slope discontinuities in the sample function.¹³

A GVT of certain types of vehicles, such as lightweight structures, requires careful attention to ensure that high levels of variability in the data do not result. One problematic issue is the effect of introducing relatively significant amounts of mass by installing sensors. This issue can be avoided by using a small set of stationary sensors but applying excitation from an impact hammer at various locations.

A susceptibility to nonlinearities potentially exists if one accelerometer is used and the impact hammer roams. Questions may exist as to stiffness of joints between components when test points straddle these joints. This problem is particularly evident with certain types of structural elements. For example, consider a bonded joint of a composite structure. This joint probably is not purely linear. If one accelerometer is placed at the tip of a composite test structure and the hammer roams across several bonded joints, that input pulse can be translated through each joint differently and the accelerometer response will show a frequency shift from one test point to the other.

Nonlinearities are an inherent part of the dynamics for any structure. These nonlinearities should be considered as a potential source for variability in the data in any test. Sources of nonlinear behavior could include springs, damping elements, boundary conditions, fluid-structure interaction, mechanical backlash in mating parts, and nonlinear electric and magnetic forces. A wide range of variability in the data, such as frequency and amplitude shifts in peaks, can result from these nonlinearities.

Variability in Analyzing Data

The purpose of a GVT is to estimate a set of properties, such as natural frequencies and mode shapes, of a structure by analyzing GVT data. Checks for coherence, reciprocity, force spectrum, and FRF quality are evaluated from the data before parameter estimation; however, these data always have some level of variability from testing issues as discussed in the previous section. Assuming the initial checks indicate the data are reasonable, the FRF data are processed using a variety of techniques that allow development of a modal model containing the mode shapes and associated frequencies. The modal parameter estimation routines are mathematical optimizations that introduce another level of variability that should be considered in the results from a GVT.

“Modal parameter estimation” refers to applying mathematical procedures for extracting eigenvalues and eigenvectors from the measured structural response. If FRFs are not consistent in the description of the poles because of variability in the test setup, applying a modal parameter estimation technique could magnify frequency and damping shifts more than are seen in the measured FRF. Many techniques are available for modal parameter estimation. The modal parameter estimation technique is selected based on the data quality and type of structural response measured. Numerous options

exist in selecting which modal parameter estimation technique is used to fit the measured data and whether time- or frequency-domain techniques are used. Sometimes multiple extraction techniques can be applied to the same data to determine how much variation occurs in the extraction.

Several techniques are conceptually similar and are sometimes grouped into categories of local, global, and polyreference approaches. The techniques considered in this paper are based on analysis of frequency-domain FRF data; however, many approaches are based on analysis of time-domain data.

The concept of a local curve fit is to analyze an individual FRF measurement and extract natural frequencies of observed modes. Corresponding mode shapes are then determined by noting the magnitude of vibration at that modal frequency at different test points. The concept of a global curve fit is to simultaneously extract the natural frequency and mode shape associated with modes by analyzing all or a subset of available FRF measurements. These techniques compute the modal properties in reference to a single FRF that represents the excitation. The polyreference approaches are somewhat similar in nature to the global approaches; however, they analyze FRF measurements using multiple references rather than a single reference. Each approach has strengths and weaknesses, so analyzing data using several approaches is common.

The modal parameters estimated from measured data naturally will have some associated variability. Analyzing an FRF using a particular technique will result in a particular modal parameter; however, analyzing that same FRF using a different technique probably will result in a different modal parameter. Issues such as optimization method, norm choices for performance indices, and numerical conditioning and stability associated with different methods will affect the parameter estimate. Thus, variability of the data is inherent to the analysis of an FRF measurement.

The issue of variability can become more pronounced when considering multiple FRF measurements as compared to a single measurement. Variability will certainly exist when analyzing the same set of FRF measurements using different techniques; however, additional variability may result from having choices of sets of FRF measurements. For example, analyzing different subsets of measurements can result in different parameter estimates even if the subsets are analyzed using the same technique. Obviously, different subsets will contain slightly different measurements because of

observability, noise, and structural nonlinearities, so the analysis of these different measurements will estimate different parameters.

The amount of variability in estimates of mode shape can be easily quantified by computing a MAC.¹⁴ The MAC is a good tool for checking similarity between modal vectors. This check is performed by computing the least square deviation with respect to the 2-norm of the vectors. Consider mode shapes, v_1 and v_2 , that are estimated using different techniques. The MAC associated with these shapes is computed as M :

$$M(v_1, v_2) = ([v_1]^T [v_2])^2 / ([v_1]^T [v_1] [v_2]^T [v_2]) \quad (2)$$

The value of the MAC is a scalar that ranges between 0 and 1. The MAC will have a value of 1 if the mode shapes are the same and a value of 0 if the shapes are orthogonal. Similarly, a MAC matrix can be computed to compare sets of mode shapes that are estimated from different approaches. This matrix will have a value of 1 for a diagonal element if the methods compute an identical mode shape, and a value less than 1 if variation exists in the shape estimates.

Variability will always exist in modal parameter estimates; however, the MAC is used to reduce variability during a GVT by providing a quick check on the data. For example, a value greater than 0.9 on the diagonal and 0.05 on the off-diagonal elements generally should be achieved for correlated modes. Thus, if test data are analyzed and the MAC indicates these desired values are not obtained, then the test can be conducted again or the procedure and setup can be altered for a new test. Conversely, a MAC matrix that shows sufficient correlation between estimates indicates the test can be considered successful because, although the modal parameter estimates show variation, this variation is as small as can be reasonably expected.

Developing Uncertainty Models

The final objective of the preflight testing considered in this paper is to determine the aeroservoelastic and flutter stability properties.¹¹ The GVT helps achieve this objective by generating information that describes the structural dynamics and is used in predicting the stability properties. Thus, the data from a GVT should be analyzed with consideration for this final objective.

Flutter analysis of a flight vehicle is performed by computing the stability properties of a linear model assumed to represent the dynamics of that vehicle. A GVT generates data, such as estimates of the natural

frequencies of structural modes, that can be used to update these models. The process of model updating, even for low-order models, is challenging because of difficulties in computing the modal parameters that represent the dynamics. The data from a test, as outlined in the previous section, have an inherent level of variation that affects the complication.

Consider the problem of computing the optimal value of natural frequency from a set of estimates with variation. Assume that this optimal value for frequency, f^* , is to be formulated using a norm approach on the data given by $\{f_1, \dots, f_n\}$. Furthermore, assume that the values are arranged in value of magnitude such that $f_1 \leq \dots \leq f_n$. The most common approach is to compute a value for f^* , that is optimal in that it minimizes the functional of $f(\cdot)$.

$$f(\cdot) = \left\| \begin{array}{c} f_1 \\ \vdots \\ f_n \end{array} \right\| \quad (3)$$

The concept of optimal for the parameter estimation is inherently tied to the concept of a norm for this type of computation. Essentially, different values for f^* will be optimal with respect to different norms used in the functional. The standard norms that are used are the 1-norm, 2-norm, and the ∞ -norm. Deriving the value for f^* that minimizes the functional for each type of norm is straightforward (table 1).

Table 1. Optimal values of frequency with respect to different norms.

Norm	
1	Median (f_1, \dots, f_n)
2	Mean (f_1, \dots, f_n)
∞	$1/2 (f_1 + f_n)$

Traditional estimates from a GVT use the 2-norm functional to choose the optimal value of natural frequency. These estimates are reasonable choices to update models used for traditional flutter analysis; however, the ∞ -norm functional can easily be shown to be the best choice when considering robust flutter analysis.

Consider the representation of natural frequency for a model in the framework for robust flutter analysis. This framework considers the natural frequency parameter actually to be represented as a set of frequency parameters, \mathbf{f} . The set can be described by a nominal value, f^* , and a set of perturbation operators, Δ , in an additive relationship:

$$\mathbf{f} = \{ f^* + \Delta \} \quad (4)$$

The uncertain model, unlike the traditional model, requires two parameters, f^* and Δ , to be chosen from the GVT data. This data analysis problem is actually quite different from the traditional problem that was solved by minimizing $f(\cdot)$. Essentially, robust flutter analysis is not predominately concerned with stability of the modes as represented by f ; instead, the analysis considers the stability with respect to the modes as represented by all values of \mathbf{f} . Thus, the data analysis must address a functional that depends on the set of natural frequencies in \mathbf{f} .

The fundamental nature of robust flutter analysis is to compute a worst-case margin for stability with respect to an uncertainty description. This margin can be highly sensitive to the size of the uncertainty; therefore, the uncertainty description should be as small as possible to reduce conservatism in the robustness analysis. This goal immediately presents the functional that should be used for analysis of GVT data: namely, the data should be analyzed to compute a natural frequency with the smallest associated uncertainty description that consequently results in the least-conservative robust flutter speed.

The set, \mathbf{f} , is used to represent the natural frequency and its uncertainty. Thus, the optimal value of f^* is to choose f^* as the range of measurements in the GVT data. The range of Δ should match, but not exceed, the range of variability noted in the data. Any values of Δ that lie outside the range of data measurements would constitute extra uncertainty and cause the flutter speed to be overly conservative. Conversely, any data measurements that lie outside the range of Δ would not be considered in the robustness analysis and cause the flutter speed to be suspect.

The main concept used to compute the parameters, f^* and Δ , of the optimal \mathbf{f} is to note the symmetric nature of this set. The values of Δ are determined by a symmetric set of norm-bounded uncertainties that affect a nominal value. Such an uncertainty description does not have any bias in the sense that the set, Δ , contains the same number of small perturbations and large

perturbations. This symmetric nature, coupled with the desire to have σ match the range of data, indicates that the optimal value of σ is in the middle of the data measurements and σ is one-half the size of the data variations. More specifically, σ can be computed using the smallest and largest values, x_1 and x_n , of the set of measurements:

$$\sigma = \{ (x_n + x_1)/2, \| (x_n - x_1)/2 \} \quad (5)$$

The range of σ clearly matches the range of the data measurements. Also, the value of σ that results in this optimal range of σ is the value that results from using the ∞ -norm as noted in table 1. The ∞ -norm, rather than the traditional 2-norm, is thus shown to be the optimal choice to analyze GVT data for robust flutter analysis.

A small example serves to show that computing using an ∞ -norm approach results in the smallest range for σ . Assume that four data estimates are to be considered as possibly representative of the true natural frequency. These estimates are $\{19, 20, 21, 25\}$. Table 2 shows the nominal value and uncertainty description, along with the resulting range given by σ , for different norm functionals.

Table 2. Analysis of example data.

Norm			
1	20.50	4.50	[16.00, 25.00]
2	21.25	3.75	[17.50, 25.00]
	22.00	3.00	[19.00, 25.00]

The range of the uncertain parameter, σ , is smallest when analyzing the data using the ∞ -norm functional. Note that this result is in contrast to traditional methods that always compute the optimal parameter using a weighted 2-norm approach. The important consideration here is that the data are not being analyzed to compute the optimal flutter solution; rather, the data are being analyzed to compute the least-conservative robust flutter solution.

Experimental Test Bed

An experimental test bed has been used to examine the flutter prediction methods of the flutterometer. The following sections examine the construction of the test bed, the GVT, modal analysis, data correlation, the uncertainty model, and robust flutter analysis.

Description

A structure called the Aerostructures Test Wing (ATW) is being used at NASA Dryden Flight Research Center (Edwards, California) as a test bed for investigating preflight and on-line methods of predicting the onset of flutter. The ATW operates in a realistic flight environment by using an F-15 aircraft and an associated flight test fixture (FTF). The FTF is a host carrier that rests under the center of the fuselage behind the engine intakes (fig. 1).



Figure 1. F-15 aircraft with flight test fixture.

The ATW mounts horizontally to the side of this carrier for flight tests. Figure 2 shows the ATW.

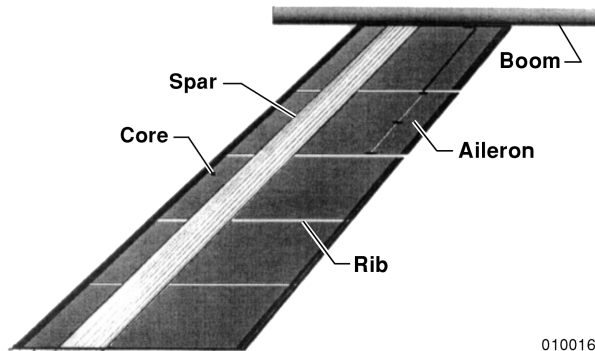


Photograph courtesy of Starr Potter.

Figure 2. Aerostructures Test Wing.

The ATW has three main components: a body, an aileron, and a boom. Because testing a wing that is more realistic and complex than solid or hollow models

is desired, the body is designed with an internal rib and spar structure (fig. 3).



010016

Figure 3. ATW internal assembly.

The aileron will allow active control of the system; however, it has been glued in the faired position for the purposes of the initial flutter testing. The boom is a hollow tube with lumped masses that induces a flutter instability at a desired flight condition.

The ATW was constructed to have a NACA-65A004 airfoil shape. The dimensions were determined by balancing desires to make the test bed large enough to be useful with consideration of safety-of-flight restrictions associated with flight operations. Table 3 shows ATW dimensions.

Table 3. Parameters of the ATW.

Parameter	Value
Airfoil	NACA-65A004
Half span	18 in.
Root chord	13.2 in.
Tip chord	8.7 in.
Semispan area	197 in ²
Aspect ratio	3.28
Span	20 percent ($\pm 10^\circ$)
Twist	+3° wash-in at tip
Taper ratio	0.659
Sweepback at quarter chord	45°

Note the positive value of 3° wash-in at the tip of the wing (table 3). The original design called for 3° washout at the tip; however, construction errors resulted

in a positive angle of twist. This error caused some concern regarding aerodynamic and divergence issues, but these concerns were alleviated by mounting the entire ATW to the FTF at an angle of -4° . This angle will minimize the steady static aerodynamic loads for bending and torsion of the ATW measured at the wing root and the spar centerline.

The materials used to construct the ATW were chosen to satisfy safety-of-flight issues for the F-15 airplane and the FTF. In particular, concern existed that a heavy piece of metal could damage the aircraft system if the ATW undergoes a flutter. This concern was addressed by building the ATW out of lightweight materials with no metal pieces. Composites and fiberglass were used for many elements, and foam was used for the internal core. The mass in the boom is provided by powdered metal to minimize risk if the boom strikes the aircraft. Table 4 shows the materials used in the ATW construction.

Table 4. Materials used in the ATW.

Elements	Materials
Skin, spar web, aileron	Fiberglass cloth and epoxy
Spar cap, boom	Carbon fiber and epoxy
Wing core	Rigid foam
Mass balance material	Powdered tungsten carbide

The mass of the ATW is an issue that is closely related to the materials. The onset of a flutter instability could cause the ATW to break near the root and allow the entire ATW to hit the F-15 airplane. The materials of the ATW are designed to be frangible and light, so this occurrence would have minimal damage. Table 5 shows the weight of the ATW and associated mass used for balancing.

Table 5. Mass properties of the ATW.

Measure	Weight, lb
Mass balance	0.65
Structure	2.00
Total	2.65

A measurement and excitation system has been incorporated into the ATW. The measurement system consists of 16 strain gages and 2 accelerometers placed throughout the wing and boom assembly. The excitation system consists of several patches of lead

zirconate titanate (piezoelectric) materials that are used to introduce sinusoidal sweeps of energy across a wide range of frequencies.

A finite-element model has been formulated to represent the ATW dynamics. The model is composed of 446 elements. This initial model has been generated from theoretical analysis of the wing design and does not include any updates from the GVT. Table 6 shows the primary modes of interest of the structural dynamics and their associated frequencies for this initial model.

Table 6. Modes of the ATW model.

Mode	Description	Frequency, Hz
1	First bending	14.50
2	First torsion	23.34
3	Second bending or torsion	84.65

The flutter mechanism for the ATW is somewhat complex. The first bending and torsion modes are coupling to provide flutter; however, a contribution from a third mode also exists, composed of a coupled bending and torsion dynamic, that needs to be included in the analysis. Computational approaches, such as p-k analysis, predict flutter to occur at a flight condition of 433 knots equivalent airspeed (*KEAS*) and an altitude of 10,500 ft at Mach 0.8.

Ground Vibration Tests

For ground testing, the ATW was rigidly mounted by clamping the wing root into the FTF plate, which was then bolted to a steel ground test fixture. Three reference accelerometers were used to measure the structural response. Two accelerometers were permanently mounted internally to the boom near the leading and trailing edge of the ATW, and a third was mounted using wax on the ATW surface centered on the nonfunctional aileron. A calibrated impact hammer with a metal tip and an added 0.065-lb mass was used to excite the structure. Several types of tips were tested; however, the metal tip excited the input frequency spectrum best through the third mode of 77 Hz. A shaker was not used for this test because the instrumentation to support a shaker test increases the weight of the wing enough to shift the modal frequency.

A total of 35 test points were excited with the impact hammer and recorded at all three accelerometer locations (fig. 4).

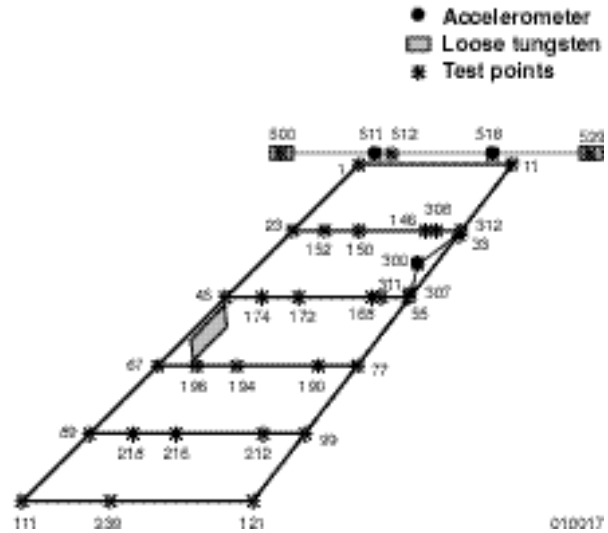


Figure 4. Locations of test points and sensors on the ATW.

These test point locations were at the leading and trailing edges, forward and aft of the spar, at the wing root and wing-to-boom joint, at accelerometer locations, and at each end of the boom near the loose mass. A large number of test points were used to ensure the GVT was able to correlate the mode shapes across the entire structure.

The data acquisition system was set up for a 200-Hz bandwidth window and 0.125-Hz resolution. No windows were used on the excitation input or on the response output because the structure is highly damped. Three responses were averaged to reduce the effects of any distortion in the recorded data.

A reciprocity test is commonly performed on a structure to ensure the GVT is properly set up. This test notes the transfer functions between two points on a structure by alternating the locations of excitation and response. Checking the reciprocity between the aft boom accelerometer (test point 518) and the wing accelerometer (test point 300) (fig. 4) showed differences in magnitude for the second and third mode and differences in damping for the third mode (fig. 5).

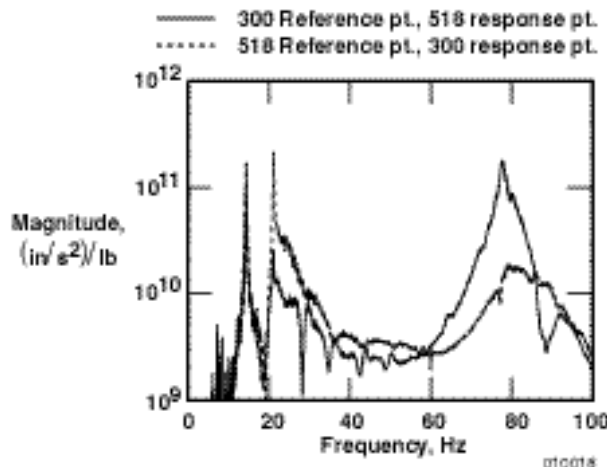


Figure 5. Transfer functions between test points 518 and 300 on the ATW.

The solid line represents the transfer function from the acceleration at point 300 to an impact excitation at point 518. The dashed line represents the transfer function from the acceleration at point 518 to an impact excitation at point 300. The functions are similar near the first mode; however, notable differences exist near the second and particularly the third mode. These differences are the first indication that an inconsistency exists because of the wing-to-boom joint or the effect of the loosely packed tungsten being located near the aft accelerometer.

Such examples of poor reciprocity are not entirely uncommon for complicated structures when using single-point to single-point analysis. The use of multiple-point excitation with multiple-point sensors can alleviate some of the effects of poor reciprocity.⁴ Thus, data analysis will consider both single- and multiple-point approaches.

Modal Analysis

Figures 6–8 show the variance in the FRF at different test locations. The appendix shows visually chosen frequency peaks for the first, second, and third modes of 29 test points measured by each accelerometer. Figures 6–8 show 29 measured FRFs, referenced from the accelerometer at point 518, to show scatter in the curves as a function of structure location. These figures graphically demonstrate the variability of the numerical

values of the handpicked frequency peaks. Every FRF test point has nearly the same frequency for the first and second modes, which draws the attention to the high variation in the third mode. Figure 6 shows five test points on the boom have a frequency variation from 78.94 to 85.00 Hz.

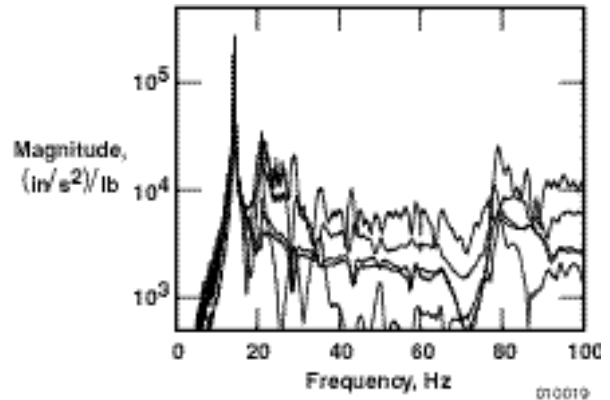


Figure 6. FRFs for five impacted boom test points recorded by the accelerometer at point 518.

Figure 7 shows nine test points on the nonfunctional aileron have a frequency variation from 77.69 to 80.44 Hz for the third mode.

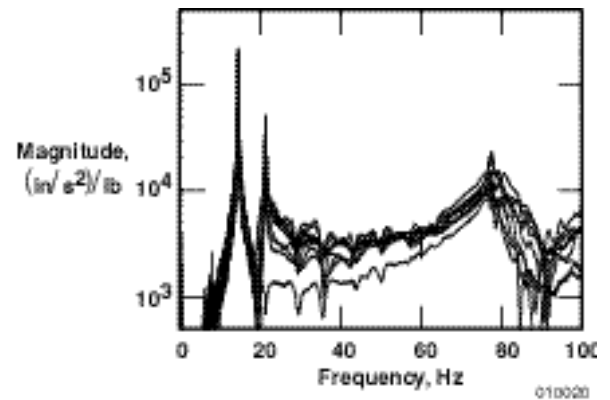


Figure 7. FRFs for nine impacted aileron test points recorded by the accelerometer at point 518.

Figure 8 shows a representative subset of test points on the ATW body, less the nonfunctional aileron and boom, that has a frequency of 77.125 Hz for the third mode.

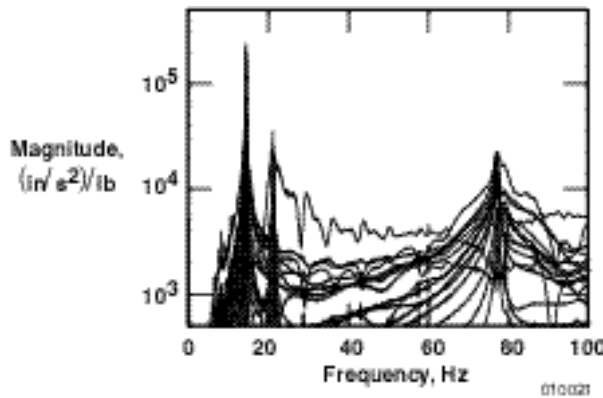


Figure 8. FRFs for a representative subset of impacted wing test points (minus the boom and glued aileron) recorded by the accelerometer at point 518.

The main issue to note from figures 6–8 is the variability in the third mode. In particular, three frequency ranges exist for the third mode, depending on the structural location of the response. Groups of accelerometers that correspond to major structural elements have been noted in several other structures to demonstrate this behavior.¹⁵ Several possible explanations for this behavior exist, such as the nonlinearity of certain elements.

Consider the nonlinearities of the ATW mass-balancing material. Located in the tips of the boom and wing leading edge are small cavities holding loosely packed, powdered tungsten (fig. 4). Speculation has been made that the loose tungsten caused a moving mass condition or that it had a frequency of its own that coupled with the third mode. In addition, the connection from the wing body to the boom (fig. 9) could have a nonlinear stiffness as a result of the adhesive bonding between the structural elements.

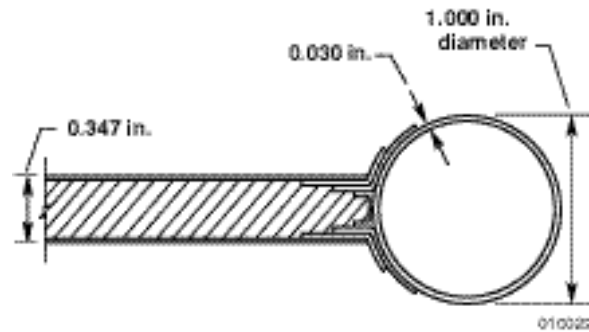


Figure 9. Wing-to-boom interface for the ATW.

Test data were analyzed for frequency and damping using local, global, and polyreference curve-fitting methods. Table 7 shows variances in frequency for each mode shape as a function of the curve-fitting technique compared with the finite-element model (FEM) and a randomly picked FRF from the appendix. Each of the curve-fitting methods used the same set of FRF data found in the appendix under point 518. The local curve-fitting method (table 7) was a single-degree-of-freedom technique that could only curve-fit the first two modes because of scatter in the third mode. The global curve-fitting method was able to fit all three modes using measured responses from the accelerometer at point 518. The polyreference curve-fitting method also fit all three modes using measured responses from the accelerometers at points 518 and 300. An orthogonal polyreference was used to provide an additional data point to describe the third mode. No trends have been found, but the polyreference curve-fitting technique presented the best results for frequency comparison with the analytical model.

Data Correlation

Table 7 shows a set of parameters that represent estimates of the natural frequencies. These estimates

Table 7. Estimates of natural frequencies.

Mode	FEM, Hz	Measured FRF peaks, Hz	Local curve-fitting, Hz	Global curve-fitting, Hz	Polyreference curve-fitting, Hz	Orthogonal Polyreference curve-fitting, Hz
1	14.50	14.43	14.34	14.23	14.51	--
2	23.34	21.06	21.03	21.30	22.28	--
3	84.65	76.81	--	77.93	77.66	78.03

were computed from modal analysis of GVT data using different techniques. Some of these estimates possibly are computed with less confidence than others; therefore, performing some correlation analysis on the data to determine its validity is important. The correlation analysis includes comparisons of test data with test data, and test data with an analytical model. Poor modal confidence factors resulting from the correlation analysis would indicate some estimates can be ignored, whereas all estimates with high modal confidence factors should be retained and used for uncertainty modeling.

Table 8 shows three modal assurance criteria to compare mode shapes as computed using different curve-fit methods. In the first method, the MAC for global curve-fitting as a function of polyreference curve-fitting was computed. In the second method, the MAC for global curve-fitting as a function of single-degree-of-freedom curve-fitting of the first two modes was computed because the local curve-fitting method could only curve-fit the first two modes. In the third method, the MAC for polyreference curve-fitting as a function of single-degree-of-freedom curve-fitting was computed, and again could only compare the first two modes. The global and polyreference approaches have the closest match to one another; the single-degree-of-freedom method becomes less effective by the second mode and can be eliminated.

Table 8. Values of MAC to compare mode shapes generated by different analysis methods.

Mode	First method	Second method	Third method
1	0.992	0.979	0.992
2	0.758	0.734	0.666
3	0.556	--	--

Comparing the global and polyreference frequencies in table 7, deciding which of the two curve-fitting techniques best compares mode shape to the FEM is difficult. The “Modal Analysis” section noted that polyreference curve-fitting shows the closest match with the FEM (comparing frequency only). Table 7 shows the polyreference technique more closely matching the FEM frequencies for the first and second modes, but the global curve fit slightly better matches the third mode of the FEM. The final choice is made when comparing the global and polyreference curve fits with the FEM using the pseudo-orthogonality check (POC), which is

sometimes referred to as self-orthogonality or cross-orthogonality.

The POC is calculated after the MAC matrix indicates valid test data and the FEM has been updated with the GVT data. This check assures that applying the analytical mass matrix to the test mode shape for correlation with the FEM will give correct results. To compare test mode shapes with analytical mode shapes, the full-degree-of-freedom analytical model was reduced to the measurement degree of freedom from test using a reduced mass matrix. The reduced mass matrix is also used for orthogonality calculations and a back expansion to fill in unmeasured degrees of freedom for better mode shape visualization.

Orthogonality is a vector-based technique that uses the analytical mass matrix that has been reduced to the set degree of freedom from test. Therefore, the accuracy of the technique depends on the accuracy of the analytical mass matrix and an appropriate number of degrees of freedom being included in the reduction process (and in the test). The POC calculation for predicted and measured eigenvectors is given as:

$$[X]^T [M_A] [A] = [X] \quad (6)$$

If the measured modes are indeed mass-normalized and orthogonal with respect to the mass matrix, $[M_A]$; the test eigenvectors, $[X]$, and the analysis eigenvectors, $[A]$, represent the same mode shapes and the orthogonality criterion, $[X]$, will be close to the identity matrix. The POC criterion places constraints on $[X]$ that the values of the diagonal should be in excess of 0.90 and off-diagonal terms smaller than 0.05. Correlating test mode shapes to test mode shapes using the same measured data shows an unanticipated match as higher frequency modes are introduced. This match means the same test data curve-fitted slightly different than the predicted mode shape will have two different orthogonality matrices. The POC matrix with the diagonal terms closest to a value of 1.0 and the off-diagonal terms closest to a value of 0 will be used to update the FEM.

The POC in table 9 compares an analytical mode shape, ϕ , as a function of an estimated mode shape, v , as computed by a single reference (point 518 accelerometer) global curve fit. These values indicate a reasonable degree of orthogonality is achieved; however, v_3 had a relatively low comparison to the analytical model because of inadequate data collection at that mode.

Table 9. Orthogonality measures to compare analytical and global estimated mode shapes.

Estimated mode shape	Analytical mode shape		
	1	2	3
v1	0.983	0.040	0.064
v2	0.249	0.966	0.015
v3	0.322	0.420	0.676

The POC in table 10 compares the analytical mode shape as a function of the two reference (points 518 and 300) polyreference curve fits. The results in table 10 show that the test mode shape has a slightly better comparison to the FEM when information from two accelerometers are used to curve-fit. This cross-orthogonality check shows the two mode shapes similarly match enough to consider the model a reasonably accurate representation of the test data.

Table 10. Orthogonality measures to compare analytical and polyreference estimated mode shapes.

Estimated mode shape	Analytical mode shape		
	1	2	3
v1	0.992	0.015	0.018
v2	0.216	0.949	0.113
v3	0.084	0.331	0.873

The high correlation shown in tables 8–10 indicates that the GVT produced relatively consistent modal estimates. Less confidence exists in the estimates associated with the third mode than in the first and second modes; however, the data in table 7 is believed to represent a set of valid GVT data. Thus, all the estimates in table 7 will be used for uncertainty modeling and, consequently, robust flutter analysis.

Uncertainty Model

The GVT data were analyzed to derive uncertain models of the natural frequencies of the ATW. These models include a nominal value of the natural frequency and an associated uncertainty description. The nominal value and the uncertainty are formulated by analyzing the data using the functional approach described in this paper for different norms. Table 11 shows the uncertain model of the natural frequency for the first mode.

Table 11. Modal parameters for the first mode.

Norm	ω_n , Hz	σ_{ω_n} , Hz	$\omega_{n, range}$, Hz
1	14.43	0.20	[14.23, 14.64]
2	14.39	0.16	[14.23, 14.55]
	14.37	0.14	[14.23, 14.51]

The data from the GVT show variations in estimates of approximately 0.28 Hz, so the uncertain parameter, ω_n , should contain at least, but hopefully not much more than, 0.28 Hz of variation. Table 11 shows that the range of values covered by ω_n has a variation of 0.41 Hz when using the 1-norm, 0.32 Hz when using the 2-norm, and only 0.28 Hz when using the ∞ -norm.

An interesting feature of the results (table 11) is the difference in the nominal value of the optimal estimate of natural frequency, ω_n . The data are biased towards the large-value extremum of the observed range, and so the optimal estimate obtained using the 1-norm and 2-norm functionals is higher than that obtained using the ∞ -norm. The ability of the 2-norm to account for this bias accounts for its use in traditional analysis. The ∞ -norm appears to derive a skewed estimate for ω_n that does not account for the bias in the data; however, the resulting uncertainty is smaller. Thus, the ∞ -norm approach is clearly the least-conservative approach when analyzing data for the purpose of robust flutter analysis.

The estimates of natural frequency for the second mode were analyzed, and table 12 shows the results. This mode, similar to the first mode, shows that the ∞ -norm approach generates an ω_n with the least amount of range needed to match the range of experimental estimates.

Table 12. Modal parameters for the second mode.

Norm	ω_n , Hz	σ_{ω_n} , Hz	$\omega_{n, range}$, Hz
1	21.30	1.56	[19.74, 22.86]
2	21.71	1.15	[20.56, 22.86]
	21.95	0.92	[21.03, 22.86]

Table 13 gives the analysis results for the third mode. This analysis presents the same conclusion as that of the other modes; namely, the ∞ -norm approach is preferable for modeling uncertain parameters to be used in robust flutter analysis.

Table 13. Modal parameters for the third mode.

Norm	ω , Hz	ζ	ω , Hz
1	77.93	3.89	[74.04, 81.82]
2	78.45	3.37	[75.08, 81.82]
	79.32	2.50	[76.82, 81.82]

Robust Flutter Analysis

Robust flutter speeds were computed for the analytical models that contain the uncertain natural frequencies shown in tables 11–13. Table 14 shows these speeds.

Table 14. Nominal and robust flutter speeds.

Norm	V_{nom} , KEAS	V_{rob} , KEAS
1	371	317
2	384	343
	392	359

The main feature of interest in table 14 is the variation in value of the robust flutter speed,¹¹ V_{rob} . Specifically, the model based on ∞ -norm analysis has a robust flutter speed that is 42 KEAS higher than the corresponding speed computed using the 1-norm analysis. This result clearly shows that the ∞ -norm approach results in the least-conservative answer.

The reason for the decrease in conservatism can be easily discerned by examining tables 11–12. Basically, the value of ω for the first mode is allowed to be as high as 14.63 Hz when using the 1-norm analysis but only 14.51 Hz when using the ∞ -norm analysis. Conversely, the value of ω for the second mode is allowed to be as low as 19.74 Hz when using the 1-norm analysis but only 21.03 Hz when using the ∞ -norm analysis. The smaller uncertainty associated with the ∞ -norm analysis limits the size of possible frequency variations and consequently restricts the modal frequencies to being farther apart. Thus, more airspeed is needed for the modes to couple, and the robust flutter speed is higher.

Another feature to note is that the nominal flutter speed, V_{nom} , is higher for the ∞ -norm analysis than for

the other norms. This feature results from the nominal values of the natural frequencies for the first two modes being farthest apart for the ∞ -norm analysis. This result is a mere coincidence of the bias in the data. Remember that the application was actually optimizing the values to reduce the conservatism in the robust flutter speed without consideration of the nominal flutter speed. For example, the difference between the nominal flutter speeds is 21 KEAS, whereas the difference between the robust flutter speeds is 42 KEAS; so clearly the biggest advantage is seen for the robust analysis.

Conclusions

This paper considered approaches to developing uncertainty models from analysis of ground vibration test data. The objective was to formulate an uncertain value of natural frequency that represents the amount of variation observed in the test data. This paper showed that analyzing the data using an ∞ -norm approach generates a model with less uncertainty than corresponding 1-norm or 2-norm approaches. The smaller uncertainty is useful for the flight test community because the associated robust flutter speeds can be computed with less conservatism. The Aerostructures Test Wing (ATW) was used to demonstrate this procedure. A ground vibration test was performed on the ATW and used to generate a range of natural frequency estimates. These estimates were analyzed using the different norm approaches to formulate uncertainty models that cover the entire range of observed variations. The approach using the ∞ -norm produces the smallest uncertainty and the least-conservative robust flutter speed.

Appendix

This appendix provides handpicked estimates of natural frequencies that arose from different accelerometer measurements. These measurements correspond to the fixed-location accelerometers, noted as references in table A-1, in response to hammer excitations at locations described as node numbers. Note that there are only 33 points listed, whereas figure 4 indicates 35 test points. This discrepancy results from not including data from points 512 and 239, which did not provide additional information beyond these 33 points. Also note that certain entries are labeled as “NODE” to indicate that this excitation location lay along the node line for that particular mode.

Table A-1. Estimates of natural frequencies.

Reference point 511 (Forward boom accelerometer)				Reference point 518 (Aft boom accelerometer)				Reference point 300 (Aileron accelerometer)			
Point	Mode 1	Mode 2	Mode 3	Point	Mode 1	Mode 2	Mode 3	Point	Mode 1	Mode 2	Mode 3
500	14.438	21.063	80.125	500	14.438	21.063	79.563	500	14.438	21.063	79.56
511	14.438	NODE	79.25	511	14.438	21.063	79.25	511	14.438	21.375	79.25
518	14.438	21.063	79.25	518	14.438	21.063	78	518	14.438	21.063	79.68
529	14.438	22.313	78.938	529	14.438	21.063	78.938	529	14.438	21.063	78.93
1	14.438	NODE	76.5	1	14.438	NODE	NODE	1	14.438	21.375	77.125
11	14.438	21.063	79.25	11	14.438	21.063	79.25	11	14.438	21.063	77.44
23	14.438	21.375	77.125	23	14.438	21.063	76.81	23	14.438	21.063	77.125
33	14.438	21.063	78.313	33	14.438	21.063	76.81	33	14.438	21.063	77.125
152	14.438	NODE	77.125	152	14.438	21.063	76.81	152	14.438	21.063	77.125
150	14.438	NODE	77.125	150	14.438	21.063	76.81	150	14.438	21.063	77.125
146	14.438	21.375	76.813	146	14.438	21.063	77.125	146	14.438	21.063	77.125
308	14.438	21.063	77.125	308	14.438	21.063	77.125	308	14.438	21.063	77.125
312	14.438	21.063	77.125	312	14.438	21.063	77.44	312	14.438	21.063	77.44
300	14.438	21.375	77.125	300	14.438	21.063	77.125	300	14.438	21.063	79.56
307	14.438	21.063	77.125	307	14.438	21.063	77.44	307	14.438	21.063	77.44
311	14.438	21.063	77.125	311	14.438	21.063	77.125	311	14.438	21.063	77.125
55	14.438	21.375	77.688	55	14.438	21.063	77.44	55	14.438	21.063	77.44
168	14.438	21.375	77.125	168	14.438	21.063	77.125	168	14.438	21.063	77.125
172	14.438	NODE	76.813	172	14.438	21.063	77.125	172	14.438	21.063	77.125
174	14.438	21.375	77.125	174	14.438	21.063	76.81	174	14.438	21.063	77.125
45	14.438	21.375	77.125	45	14.438	21.063	77.125	45	14.438	21.063	77.125
67	14.438	21.375	77.125	67	14.438	21.063	77.125	67	14.438	21.063	77.125
196	14.438	21.375	76.81	196	14.438	21.063	77.125	196	14.438	21.063	77.125
194	14.438	21.375	77.125	194	14.438	21.063	77.125	194	14.438	21.063	77.125
190	14.438	21.375	77.125	190	14.438	21.063	76.813	190	14.438	21.063	77.125
77	14.438	21.375	77.125	77	14.438	21.063	77.125	77	14.438	21.063	77.125
89	14.438	21.375	77.125	89	14.438	21.063	77.125	89	14.438	21.063	77.125
218	14.438	21.375	76.81	218	14.438	21.063	76.81	218	14.438	21.33	77.125
216	14.438	21.375	76.81	216	14.438	21.063	76.81	216	14.438	21.33	77.125
212	14.438	NODE	76.81	212	14.438	21.063	76.81	212	14.438	21.063	77.125
99	14.438	21.063	76.81	99	14.438	21.063	76.81	99	14.438	21.063	77.125
111	14.438	21.063	77.125	111	14.438	21.063	77.125	111	14.438	21.063	77.125
121	14.438	21.063	76.813	121	14.438	21.063	76.813	121	14.438	21.063	76.81

References

- ¹Kehoe, Michael W., *Aircraft Ground Vibration Testing at NASA Ames-Dryden Flight Research Facility*, NASA-TM-88272, 1987.
- ²Natke, H. G. “Problems of Model Updating Procedures: A Perspective Resumption,” *Mechanical Systems and Signal Processing*, vol. 12, no. 1, 1998, pp. 65–74.
- ³Alampalli, S., “Effects of Testing, Analysis, Damage, and Environment on Modal Parameters,” *Mechanical Systems and Signal Processing*, vol. 14, no. 1, 2000, pp. 63–74.
- ⁴Avitabile, P., “Correlation Considerations – Part 3 (Experimental Modal Testing Considerations for Finite Element Model Correlation),” *Proceedings of the 16th International Modal Analysis Conference*, Society for Experimental Mechanics, Inc., 1998, pp. 185–196.
- ⁵Cafeo, John A., Douglas A. Feldmaier, and Spencer J. Doggett, “Considerations to Reduce Modal Analysis Test Variability,” *Proceedings of the 16th International Modal Analysis Conference*, Society for Experimental Mechanics, Inc., 1998, pp. 470–476.
- ⁶Brillhart, Ralph, Tom Deiters, and Ken Smith, “Improving Model Correlation Through Test Preparation and Conduct,” *Proceedings of the 16th International Modal Analysis Conference*, Society for Experimental Mechanics, Inc., 1998, pp. 464–469.
- ⁷Friswell, M. I., J. E. Mottershead, and T. Shenton, “Robust Model Updating,” *Proceedings of the 18th International Modal Analysis Conference*, Society for Experimental Mechanics, Inc., 2000, pp. 987–991.
- ⁸Plessis, G., B. Lallemand, T. Tison, and P. Level, “A Fuzzy Method for the Modal Identification of Uncertain Experimental Data,” *Proceedings of the 18th International Modal Analysis Conference*, 2000, pp. 1831–1837.
- ⁹Phillips, Allyn W., Randall J. Allemang, and Charles R. Pickrel, “Clustering of Modal Frequency Estimates from Different Solution Sets,” *Proceedings of the 15th International Modal Analysis Conference*, Society for Experimental Mechanics, Inc., 1997, pp. 1053–1063.
- ¹⁰Cafeo, John A., Robert V. Lust, and Ulrich M. Meireis, “Uncertainty in Mode Shape Data and its Influence on the Comparison of Test and Analysis Models,” *Proceedings of the 18th International Modal Analysis Conference*, Society for Experimental Mechanics, Inc., 2000, pp. 349–355.
- ¹¹Lind, Rick and Marty Brenner, *Robust Aeroservoelastic Stability Analysis*, Springer-Verlag, London, 1999.
- ¹²Ben-Haim, Y., S. Cogan, and L. Sanseigne, “Usability of Mathematical Models in Mechanical Decision Processes,” *Mechanical Systems and Signal Processing*, vol. 12, no. 1, 1998, pp. 121–134.
- ¹³McConnell, Kenneth G., *Vibration Testing: Theory and Practice*, John Wiley & Sons, Inc., New York, 1995, pp. 441–534.
- ¹⁴Ewins, D. J., *Modal Testing: Theory and Practice*, Research Studies Press Ltd., England, 1984, pp. 217–251.
- ¹⁵Cafeo, John A., Spencer Doggett, Douglas A. Feldmaier, Robert V. Lust, Donald J. Nefske, and Shung H. Sung, “A Design-of-Experiments Approach to Quantifying Test-to-Test Variability for a Modal Test,” *Proceedings of the 15th International Modal Analysis Conference*, Society for Experimental Mechanics, Inc., 1997, pp. 598–604.

REPORT DOCUMENTATION PAGE

Form Approved
OMB No. 0704-0188

Public reporting burden for this collection of information is estimated to average 1 hour per response, including the time for reviewing instructions, searching existing data sources, gathering and maintaining the data needed, and completing and reviewing the collection of information. Send comments regarding this burden estimate or any other aspect of this collection of information, including suggestions for reducing this burden, to Washington Headquarters Services, Directorate for Information Operations and Reports, 1215 Jefferson Davis Highway, Suite 1204, Arlington, VA 22202-4302, and to the Office of Management and Budget, Paperwork Reduction Project (0704-0188), Washington, DC 20503.

1. AGENCY USE ONLY (Leave blank)		2. REPORT DATE April 2001	3. REPORT TYPE AND DATES COVERED Technical Memorandum	
4. TITLE AND SUBTITLE Developing Uncertainty Models for Robust Flutter Analysis Using Ground Vibration Test Data			5. FUNDING NUMBERS WU 274-00-00-E8-RR-00-DDF	
6. AUTHOR(S) Starr Potter and Rick Lind				
7. PERFORMING ORGANIZATION NAME(S) AND ADDRESS(ES) NASA Dryden Flight Research Center P.O. Box 273 Edwards, California 93523-0273			8. PERFORMING ORGANIZATION REPORT NUMBER H-2452	
9. SPONSORING/MONITORING AGENCY NAME(S) AND ADDRESS(ES) National Aeronautics and Space Administration Washington, DC 20546-0001			10. SPONSORING/MONITORING AGENCY REPORT NUMBER NASA/TM-2001-210392	
11. SUPPLEMENTARY NOTES Presented at 42nd AIAA/ASME/ASCE/AHS/ASC Structures, Structural Dynamics, and Materials Conference and Exhibit, Seattle, Washington, April 16–19, 2001, AIAA-2001-1585.				
12a. DISTRIBUTION/AVAILABILITY STATEMENT Unclassified—Unlimited Subject Category 05 This report is available at http://www.dfrc.nasa.gov/DTRS/			12b. DISTRIBUTION CODE	
13. ABSTRACT (Maximum 200 words) A ground vibration test can be used to obtain information about structural dynamics that is important for flutter analysis. Traditionally, this information—such as natural frequencies of modes—is used to update analytical models used to predict flutter speeds. The ground vibration test can also be used to obtain uncertainty models, such as natural frequencies and their associated variations, that can update analytical models for the purpose of predicting robust flutter speeds. Analyzing test data using the ∞ -norm, rather than the traditional 2-norm, is shown to lead to a minimum-size uncertainty description and, consequently, a least-conservative robust flutter speed. This approach is demonstrated using ground vibration test data for the Aerostructures Test Wing. Different norms are used to formulate uncertainty models and their associated robust flutter speeds to evaluate which norm is least conservative.				
14. SUBJECT TERMS Flutter, Ground vibration test, Uncertainty			15. NUMBER OF PAGES 21	
			16. PRICE CODE	
17. SECURITY CLASSIFICATION OF REPORT Unclassified	18. SECURITY CLASSIFICATION OF THIS PAGE Unclassified	19. SECURITY CLASSIFICATION OF ABSTRACT Unclassified	20. LIMITATION OF ABSTRACT Unlimited	